ACS Catalysis

Letter

pubs.acs.org/acscatalysis

Solvent Polarity-Induced Pore Selectivity in H-ZSM-5 Catalysis

Alexey V. Kubarev, Eric Breynaert, Jordi Van Loon, Arunasish Layek, Guillaume Fleury, Sambhu Radhakrishnan, Johan Martens, and Maarten B. J. Roeffaers*

Center for Surface Chemistry and Catalysis, KU Leuven, Celestijnenlaan 200F, 3001 Leuven, Belgium

Supporting Information

ABSTRACT: Molecular-sized micropores of ZSM-5 zeolite catalysts provide spatial restrictions around catalytic sites that allow for shape-selective catalysis. However, the fact that ZSM-5 has two main pore systems with different geometries is relatively unexploited as a potential source of additional shape selectivity. Here, we use confocal laser-scanning microscopy to show that by changing the polarity of the solvent, the acid-catalyzed furfuryl alcohol oligomerization can be directed to selectively occur within either of two locations in the microporous network. This finding is confirmed for H-ZSM-5 particles with different Si/Al ratios and indicates a general trend for shape-selective catalytic reactions.

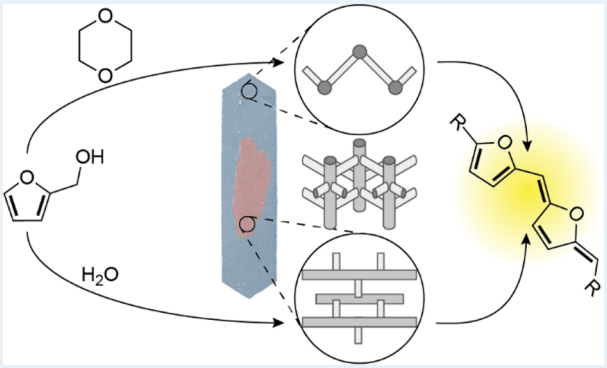

KEYWORDS: *H-ZSM-5, zeolites, confocal laser-scanning microscopy, solvent effect, pore preference*

Zeolites are the most commonly used heterogeneous catalysts in the (petro)chemical industry.[1−3] Since the middle of the 20th century, they have been extensively studied and applied in industrial processes because of their unique combination of extensive microporosity and the intrinsic strong acidity of their hydrogen form. This combination enables them to achieve both high catalytic activity and high chemical selectivity.

One of the most important and widely used types of zeolite catalysts is the hydrogen form of ZSM-5 (MFI framework type). H-ZSM-5 is industrially used in fluid catalytic cracking,[4] the synthesis of ethylbenzene,[5,6] the isomerization of xylenes,[6] and the disproportionation of toluene.[6,7] Also, it is often looked upon as the prototype of a shape-selective catalysts because of its high para-selectivity toward the alkylation of alkylbenzenes.[3] More recently, with a focus on environmentally sustainable processes, there were numerous and promising studies regarding the activity and shape selectivity of H-ZSM-5 in the catalytic conversion of biomass and its derivatives.[8−11] For example, it was shown that ZSM-5 exhibited the highest aromatic yield and the least amount of coking among 13 zeolites with different pore sizes and shapes when applied in the fast catalytic pyrolysis of glucose.[8]

The MFI framework consists of two types of intersecting 10-membered-ring pores. The geometry and size of these perpendicular pores differ: one type consists of straight channels with a size of 5.3 × 5.6 Å^2, running along the crystallographic *b*-axis, the other has a tortuous shape, commonly referred to as the sinusoidal channels, with a size of 5.1 × 5.5 Å^2, running along the crystallographic *a*-axis.[12,13] Such differences in pore size and local environment can trigger different adsorption properties between the two types of pores. For example, it has been shown that aromatic molecules, such as *p*-xylene, *p*-dichlorobenzene, and *trans*-stilbene, preferentially adsorb at different locations of the framework depending not only on the adsorbate nature but also on the adsorbate loading.[14−19] Techniques such as single-crystal X-ray diffraction and high-resolution synchrotron X-ray powder diffraction showed that at low loadings, the adsorbate molecules are preferentially located inside in the straight pores of ZSM-5 crystals,[14−16] whereas at high loadings, they accumulate at pore intersections and in the sinusoidal pores.[18,19] In addition, Eckman et al. used deuterium solid-state NMR to trace temperature-dependent changes in orientation of *p*-xylene molecules in H-ZSM-5 at low loadings. They concluded that molecules are neither able to move from the straight channels into the sinusoidal channels nor move along the sinusoidal channels.[17]

Such differences in molecular adsorption and transport should influence the catalytic processes. However, given the increased complexity of the chemical reaction system compared with adsorption and diffusion, it has proven to be not straightforward to study the molecular orientation during catalytic conversions inside zeolite crystals. Luckily, catalysis characterization has benefitted from the development and application of powerful microscopy techniques in recent years, such as fluorescence and optical microspectroscopy.[20,21] They allow the monitoring of molecular processes inside a single catalyst crystal, for example, to determine the exact location of catalytic conversions. Additionally, they can resolve the

Received: March 10, 2017
Revised: May 8, 2017
Published: May 22, 2017

DOI: 10.1021/acscatal.7b00782
ACS Catal. 2017, 7, 4248−4252

orientation of reaction products with respect to the crystalline porous network by using linearly polarized excitation light. These techniques were successfully applied to study H-ZSM-5 catalysts and their activity where other microscopic techniques failed. For example, the early attempt to use polarized Fourier-transform infrared microscopy to study the location of adsorbates in single ZSM-5 crystals was hampered by crystal twinning or intergrowth, which could not be resolved by infrared microscopy.[22] Later on, numerous fluorescence, optical and electron microscopic investigations discerned the intergrowth structure of ZSM-5 crystals and the crystallographic orientation of the subcrystal units.[23−28]

In the case of the ZSM-5 crystals used in this study, a pronounced intergrowth is present in the main body of the coffin-shaped H-ZSM-5 particles (Figure 1a). Such 90 deg intergrowths are commonly observed in ZSM-5 crystals and were previously also observed in this specific sample.[26,28] The crystallographic *c*-axis aligns with the longest particle dimension both for the main crystal body and the intergrowth. However, in the intergrowth (pink area in Figure 1a) the crystallographic *a*- and *b*-axes are rotated 90° around the *c*-axis with respect to the main crystal body (blue area in Figure 1a). As a consequence, the orientation of the straight and sinusoidal pores is swapped between the main body and the intergrowth of the crystal. This property can be exploited to reveal differences in reactivity between the two pore structures, as the orientation of the acid-catalyzed reaction products can be identified by using linear polarized excitation light (see below). Because pore systems are oriented perpendicularly to each other, differences in reactivity should be easy to identify.

As mentioned earlier, it has been described in the literature that the pore preference of *p*-dichlorobenzene depends on the adsorbate loading.[14,18] On this basis, we speculated that it should be possible to affect the pore preference of the catalytic reaction and direct the reaction to predominantly happen in one of both pore types. Numerous microspectroscopic studies have been conducted in the past to investigate the factors affecting catalytic activity of H-ZSM-5, such as its relation with the subcrystalline intergrowth structure,[24−26,29−33] the effect of commonly applied steaming treatments,[34,35] the mechanisms of coke formation,[36] and the solvent effect.[37] In particular, the choice of solvent has been shown to significantly affect the catalytic activity of H-ZSM-5 crystals in the styrene dimerization reaction, as solvents with a different polarity interact differently with zeolite Brønsted acid sites.[37] On the basis of these considerations, we hypothesized that by using different solvents the pore preference of a catalytic reaction could also be affected.

In this work, this hypothesis was investigated by comparing the effect of a polar solvent, water, to that of the more apolar, 1,4-dioxane. Earlier, both of these solvents were shown to be appropriate to study acid zeolite catalysis with our chosen probe reaction (i.e., the furfuryl alcohol oligomerization),[24,38] but they differ significantly in polarity (spectroscopic polarity indices are 1.000 for water, 0.164 for 1,4-dioxane, and 0.605 for furfuryl alcohol).[39]

We applied the furfuryl alcohol oligomerization as model reaction (Figure 1b) which catalytically stains zeolite crystals with fluorescent products. Subsequently, confocal laser-scanning (CLS) microscopy detects these fluorescent reaction products, enabling a differentiation between zones within single H-ZSM-5 crystals based on their catalytic performance (Figure 1b). The molecular orientation of the fluorescent reaction

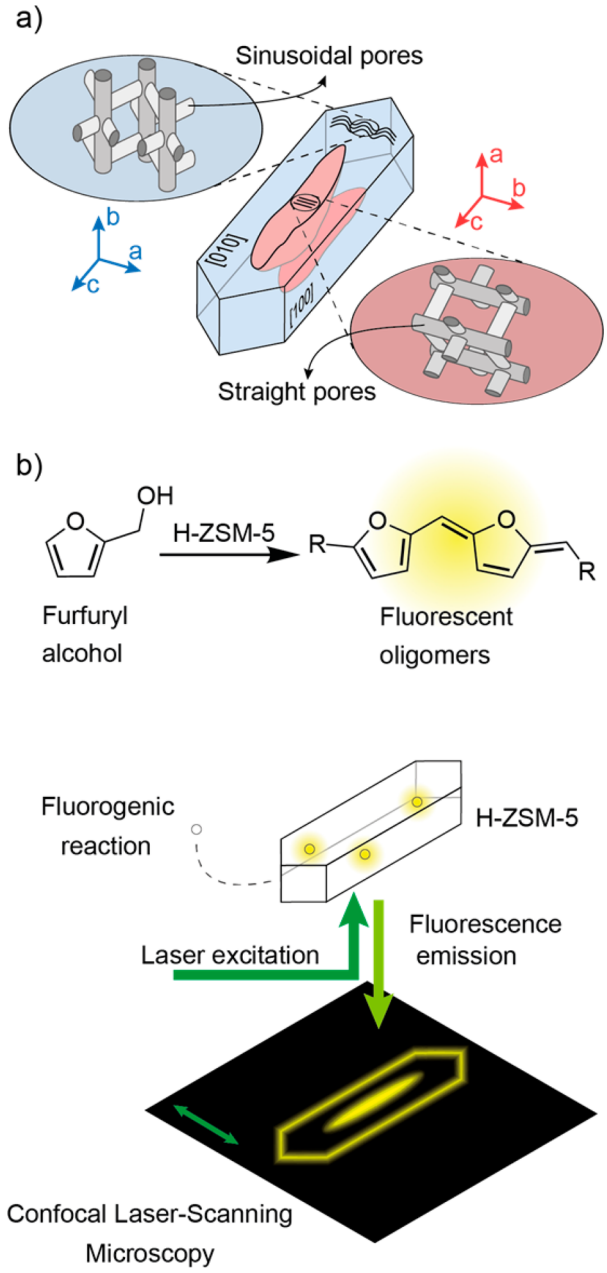

Figure 1. Schematic representation of (a) the intergrowth structure of a ZSM-5 crystal and the relative pore orientations and (b) the used fluorescence microscopy approach. The green two-headed arrow indicates the orientation of the applied light polarization.

products, and therefore the type of pore in which they are formed, was revealed using linearly polarized excitation light. Under these conditions, only fluorescent species with their dipole moment oriented along the polarization direction of the incident light (indicated by the green two-headed arrow on the figures) are efficiently excited.

In our experiments, we used four H-ZSM-5 samples with experimentally determined Si/Al ratios of 880, 82, 75, and 27, respectively, designated H-ZSM-5-880, H-ZSM-5-82, H-ZSM-5-75, and H-ZSM-5-27. In the main article, we present experimental data related only to the H-ZSM-5-880 sample, whereas the results for other samples are given in the Supporting Information.

DOI: 10.1021/acscatal.7b00782
ACS Catal. 2017, 7, 4248−4252

The CLS micrographs of the catalytically stained H-ZSM-5–880 crystals lying on their [010] plane surfaces (based on the crystallographic structure of the main body) are presented in Figure 2. In this orientation, the main crystal body has

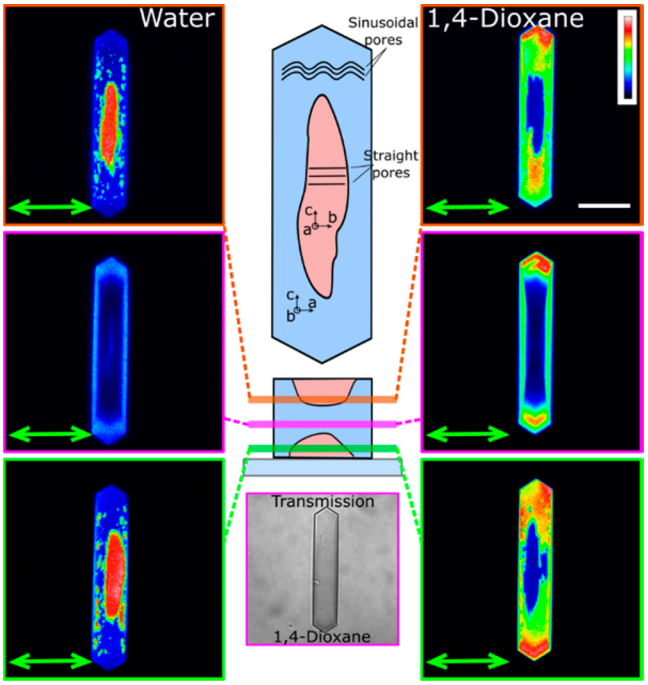

Figure 2. CLS micrographs of furfuryl alcohol oligomers accumulated at different depths within H-ZSM-5–880 crystals (lying on the [010] facet) using water (left) or 1,4-dioxane (right) as a solvent. Transmission image is presented from the 1,4-dioxane-based experiment. False color scale shows the observed fluorescence intensity adjusted for each slide; the green two-headed arrow indicates the excitation light polarization orientation; scale bar: 20 μm.

sinusoidal pores running parallel compared to the excitation light polarization orientation, while its straight pores run perpendicular to the presented image plane and lie along the direction of the light propagation. In the intergrowth, the opposite is true—the straight pores are coaligned with the excitation light polarization orientation, while the sinusoidal pores lie along the line of observation. We observed that fluorescent molecules are accumulated in the straight pores of the intergrowth when water is used as solvent, whereas reactions take place in the sinusoidal pores in the main body of the crystal in 1,4-dioxane. We conclude that, in line with our expectations, the type of pores in which the reaction takes place can be controlled on the basis of the solvent.

However, it is possible that our observations highlight differences in activity between the intergrowth and main body of the crystal, rather than between the straight and sinusoidal pores. In order to confirm our results, we have conducted CLS microscopic imaging of crystals lying on their [100] facet (based on the crystallographic structure of the main body). In this orientation, the straight pores of the main body and sinusoidal pores of the intergrowth are coaligned with the excitation light polarization orientation. The micrographs presented in Figure 3 confirm that without regard to main body or intergrowth 1,4-dioxane promotes catalytic activity in sinusoidal pores, whereas water promotes the reaction to occur mainly in the straight pores.

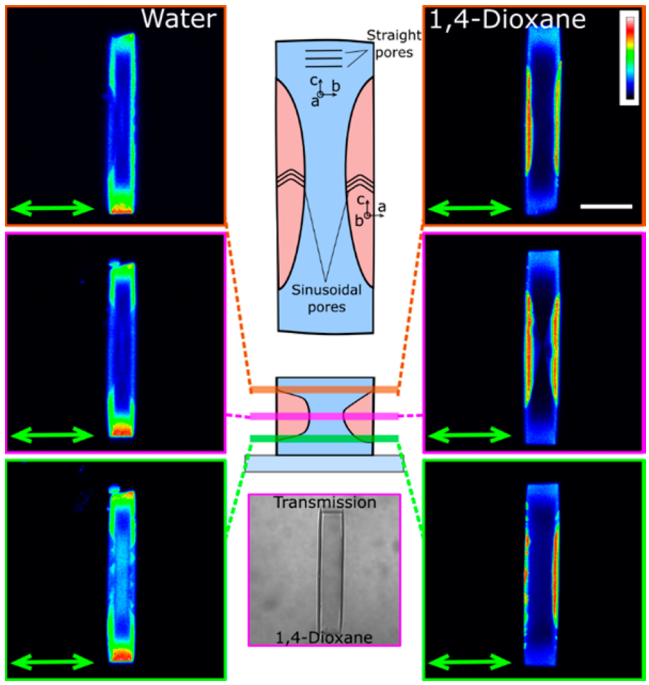

Figure 3. CLS micrographs of furfuryl alcohol oligomers accumulated at different depths within H-ZSM-5-880 crystals (lying on the [100] facet) using water (left) or 1,4-dioxane (right) as a solvent. Transmission image is presented from the 1,4-dioxane based experiment. False color scale shows the observed fluorescence intensity adjusted for each slide; the green two-headed arrow indicates the excitation light polarization orientation; scale bar: 20 μm.

We observed the same effect in two other batches: H-ZSM-5-82 and H-ZSM-5-27 (Figures S1–S4). H-ZSM-5-75 showed a slightly deviating picture. While the reaction is also highly favored in the straight pores when using water as a solvent, the product formation shows a weak preference toward the straight pores as well when 1,4-dioxane is used (Figures S5–S6).

A possible explanation for the observed solvent-dependent pore preference may be sought in the differences in solvent polarity and its interaction with the zeolite pores of different polarity. Pore polarity differences can be caused by (1) the uneven distribution of framework aluminum and the associated acid sites or (2) by differences in defect silanols in straight versus sinusoidal pores. As the pore preference effect appears to be independent of the Si/Al ratio and is even observed in Al-poor H-ZSM-5-880 sample, we rule out that framework aluminum distribution is the main cause for polarity differences. To investigate the possibility of silanol groups affecting pore polarity, we have conducted ^{1}H MAS NMR investigation of H-ZSM-5-880 (Supporting Information and Figures S8–S10),[40] which revealed an estimated minimal concentration of silanol groups as Si/SiOH ratio of 82. The actual silanol concentration is even higher as even in the calcined sample traces of water were present; water in exchange with silanols decreases the detected silanol signal. This concentration of silanols is in line with earlier reports.[41,42] Controlled addition of water shows the strong interaction with these silanols indicative for a high local polarity. From these ^{1}H MAS NMR data in combination with the CLS microscopy observations we conclude that there is a silanol-induced polarity, which is potentially different between the sinusoidal and straight pores with silanols being preferentially present in the sinusoidal pores. Hence, the

DOI: 10.1021/acscatal.7b00782
ACS Catal. 2017, 7, 4248–4252

enhanced polarity of the sinusoidal pores compared with the straight pores can lead to differences in the respective coadsorption dynamics for solvent-furfuryl alcohol systems: the more polar molecules in the system will preferentially adsorb in the sinusoidal pores and the more apolar in the straight pores. This preferential molecular absorption was further confirmed by the distribution of the apolar benzonitrile molecules, which are preferentially adsorbed along the straight pores of the H-ZSM-5-880 as revealed by stimulated Raman scattering (SRS) microscopy (Figure S11).

To further support this model that the acid catalysis in ZSM-5 is strongly influenced by differences in pore polarity and the preferential molecular adsorption, we tested another apolar solvent 2-butanone, similar in polarity to 1,4-dioxane. With a spectroscopic polarity index of 0.327, 2-butanone is more apolar than furfuryl alcohol.[39] The results of these experiments are presented in Figure 4. The measured catalytic activity

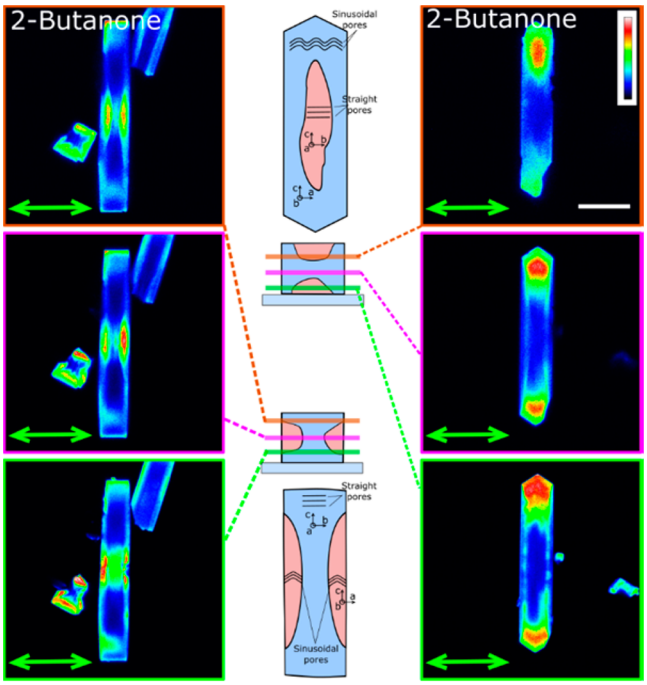

Figure 4. CLS micrographs of furfuryl alcohol oligomers accumulated at different depths within H-ZSM-5-880 crystals lying on the [100] (left) and [010] (right) facet using 2-butanone as a solvent. False color scale shows the observed fluorescence intensity adjusted for each slide; the green two-headed arrow indicates the excitation light polarization orientation; scale bar: 20 μm.

patterns confirm that the activity is mostly restricted to sinusoidal pores of H-ZSM-5, similar to the reaction in 1,4-dioxane and opposite to what is observed in water. These results support our proposed model that the observed solvent-induced pore preference is indeed guided by the solvent polarity and the related molecular adsorption based on pore polarity.

In conclusion, the presented work shows that differences in solvent and reagent polarity can be employed to steer the catalytic activity toward the straight or sinusoidal pores in H-ZSM-5. This effect is likely related to the intrinsic presence of silanol defects. CLS microscopy in combination with furfuryl alcohol oligomerization as probe reaction shows that this acid catalyzed reaction preferentially occurs in the straight pores of H-ZSM-5 crystals if water is used as solvent and in the sinusoidal pores if the more apolar 1,4-dioxane or 2-butanone are used. Additional ^{1}H MAS NMR spectroscopy and SRS microscopy with probe molecules support the proposed model, which relates the observed pore preference to a difference in polarity between straight and sinusoidal pores as result of silanol defects.

■ ASSOCIATED CONTENT

Supporting Information

The Supporting Information is available free of charge on the ACS Publications website at DOI: 10.1021/acscatal.7b00782.

Experimental details about the used materials, sample preparation, and experiments; the CLS micrographs of catalytically stained samples H-ZSM-5-82, H-ZSM-5-75, and H-ZSM-5-27; the results of thermogravimetric analysis of catalytically stained H-ZSM-5-880; the results of ^{1}H MAS NMR spectroscopy study of H-ZSM-5-880; the results of SRS microscopy investigation of benzonitrile adsorption in H-ZSM-5-880 (PDF)

■ AUTHOR INFORMATION

Corresponding Author

*E-mail: maarten.roeffaers@kuleuven.be.

ORCID

Eric Breynaert: 0000-0003-3499-0455
Arunasish Layek: 0000-0003-2435-4009
Maarten B. J. Roeffaers: 0000-0001-6582-6514

Notes

The authors declare no competing financial interest.

■ ACKNOWLEDGMENTS

The authors thank Collin Tan Yong Xiang for the assistance with thermogravimetric analysis. The authors acknowledge financial support from the Research Foundation Flanders (FWO, Grant No. G.0962.13, G.0197.11, and G.0885.14N), the KU Leuven Research Fund (C14/15/053), and the Hercules foundation (HER/11/14, AKUL/13). The research leading to these results has received funding from the European Research Council under the European Union's Seventh Fremwork Programme (FP/2007-2013)/ERC Grant Agreement No. [307523], ERC-Stg LIGHT to M.B.J.R.

■ REFERENCES

(1) Mizuno, N.; Misono, M. *Chem. Rev.* **1998**, *98*, 199−218.
(2) Čejka, J.; Centi, G.; Perez-Pariente, J.; Roth, W. J. *Catal. Today* **2012**, *179*, 2−15.
(3) Weitkamp, J. *Solid State Ionics* **2000**, *131*, 175−188.
(4) Degnan, T. F.; Chitnis, G. K.; Schipper, P. H. *Microporous Mesoporous Mater.* **2000**, *35*−*36*, 245−252.
(5) Abichandani, J. S.; Beck, J. S.; McCullen, S. B.; Olson, D. H. Ethylbenzene production process with ex situ selectivated zeolite catalyst. U.S. Patent 5689025 A, 1995.
(6) *Catalysis and Zeolites*; Weitkamp, J., Puppe, L., Eds.; Springer: Berlin, Heidelberg, 1999.
(7) Kaeding, W. *J. Catal.* **1981**, *69*, 392−398.
(8) Jae, J.; Tompsett, G. A.; Foster, A. J.; Hammond, K. D.; Auerbach, S. M.; Lobo, R. F.; Huber, G. W. *J. Catal.* **2011**, *279*, 257−268.
(9) González Maldonado, G. M.; Assary, R. S.; Dumesic, J.; Curtiss, L. A. *Energy Environ. Sci.* **2012**, *5*, 6981−6989.
(10) Mellmer, M. A.; Gallo, J. M. R.; Martin Alonso, D.; Dumesic, J. A. *ACS Catal.* **2015**, *5*, 3354−3359.

DOI: 10.1021/acscatal.7b00782
ACS Catal. 2017, 7, 4248−4252

(11) Lima, T. M.; Lima, C. G. S.; Rathi, A. K.; Gawande, M. B.; Tucek, J.; Urquieta-González, E. A.; Zbořil, R.; Paixão, M. W.; Varma, R. S. *Green Chem.* **2016**, *18*, 5586−5593.
(12) Kokotailo, G. T.; Lawton, S. L.; Olson, D. H.; Meier, W. M. *Nature* **1978**, *272*, 437−438.
(13) Olson, D. H.; Kokotailo, G. T.; Lawton, S. L.; Meier, W. M. *J. Phys. Chem.* **1981**, *85*, 2238−2243.
(14) van Koningsveld, H.; Jansen, J. C.; de Man, A. J. M. *Acta Crystallogr., Sect. B: Struct. Sci.* **1996**, *52*, 131−139.
(15) Parise, J. B.; Hriljac, J. A.; Cox, D. E.; Corbin, D. R.; Ramamurthy, V. *J. Chem. Soc., Chem. Commun.* **1993**, *3*, 226−228.
(16) Gies, H.; Marler, B.; Fyfe, C.; Kokotailo, G.; Feng, Y.; Cox, D. E. *J. Phys. Chem. Solids* **1991**, *52*, 1235−1241.
(17) Eckman, R. R.; Vega, A. J. *J. Phys. Chem.* **1986**, *90*, 4679−4683.
(18) van Koningsveld, H.; Jansen, J. C.; van Bekkum, H. *Acta Crystallogr., Sect. B: Struct. Sci.* **1996**, *52*, 140−144.
(19) van Koningsveld, H.; Tuinstra, F.; van Bekkum, H.; Jansen, J. C. *Acta Crystallogr., Sect. B: Struct. Sci.* **1989**, *45*, 423−431.
(20) Janssen, K. P. F.; De Cremer, G.; Neely, R. K.; Kubarev, A. V.; Van Loon, J.; Martens, J. A.; De Vos, D. E.; Roeffaers, M. B. J.; Hofkens, J. *Chem. Soc. Rev.* **2014**, *43*, 990−1006.
(21) Weckhuysen, B. M. *Angew. Chem., Int. Ed.* **2009**, *48*, 4910−4943.
(22) Schueth, F. *J. Phys. Chem.* **1992**, *96*, 7493−7496.
(23) Roeffaers, M. B. J.; Sels, B. F.; Uji-i, H.; Blanpain, B.; L'hoëst, P.; Jacobs, P. A.; De Schryver, F. C.; Hofkens, J.; De Vos, D. E. *Angew. Chem., Int. Ed.* **2007**, *46*, 1706−1709.
(24) Roeffaers, M. B. J.; Ameloot, R.; Baruah, M.; Uji-i, H.; Bulut, M.; De Cremer, G.; Müller, U.; Jacobs, P. A.; Hofkens, J.; Sels, B. F.; De Vos, D. E. *J. Am. Chem. Soc.* **2008**, *130*, 5763−5772.
(25) Karwacki, L.; Stavitski, E.; Kox, M. H. F.; Kornatowski, J.; Weckhuysen, B. M. *Stud. Surf. Sci. Catal.* **2008**, *174*, 757−762.
(26) Roeffaers, M. B. J.; Ameloot, R.; Bons, A.-J.; Mortier, W.; De Cremer, G.; de Kloe, R.; Hofkens, J.; De Vos, D. E.; Sels, B. F. *J. Am. Chem. Soc.* **2008**, *130*, 13516−13517.
(27) Stavitski, E.; Drury, M. R.; De Winter, D. A. M.; Kox, M. H. F.; Weckhuysen, B. M. *Angew. Chem., Int. Ed.* **2008**, *47*, 5637−5640.
(28) Karwacki, L.; Kox, M. H. F.; de Winter, D. A. M.; Drury, M. R.; Meeldijk, J. D.; Stavitski, E.; Schmidt, W.; Mertens, M.; Cubillas, P.; John, N.; Chan, A.; Kahn, N.; Bare, S. R.; Anderson, M.; Kornatowski, J.; Weckhuysen, B. M. *Nat. Mater.* **2009**, *8*, 959−965.
(29) Kox, M. H. F.; Stavitski, E.; Groen, J. C.; Pérez-Ramírez, J.; Kapteijn, F.; Weckhuysen, B. M. *Chem. - Eur. J.* **2008**, *14*, 1718−1725.
(30) Roeffaers, M. B. J.; Sels, B. F.; De Schryver, F. C.; Jacobs, P. A.; Hofkens, J.; De Vos, D. E. In situ filming of reactions inside individual zeolite crystals using fluorescence microscopy. In *Stud. Surf. Sci. Catal.*; Xu, R., Gao, Z., Chen, J., Yan, W., Eds.; Elsevier: Amsterdam, 2007; Vol. *170*, pp 717−723.
(31) Kox, M. H. F.; Stavitski, E.; Weckhuysen, B. M. *Angew. Chem., Int. Ed.* **2007**, *46*, 3652−3655.
(32) Stavitski, E.; Kox, M. H. F.; Weckhuysen, B. M. *Chem. - Eur. J.* **2007**, *13*, 7057−7065.
(33) Sprung, C.; Weckhuysen, B. M. *J. Am. Chem. Soc.* **2015**, *137*, 1916−1928.
(34) Aramburo, L. R.; Teketel, S.; Svelle, S.; Bare, S. R.; Arstad, B.; Zandbergen, H. W.; Olsbye, U.; de Groot, F. M. F.; Weckhuysen, B. M. *J. Catal.* **2013**, *307*, 185−193.
(35) Ristanović, Z.; Hofmann, J. P.; De Cremer, G.; Kubarev, A. V.; Rohnke, M.; Meirer, F.; Hofkens, J.; Roeffaers, M. B. J.; Weckhuysen, B. M. *J. Am. Chem. Soc.* **2015**, *137*, 6559−6568.
(36) Mores, D.; Stavitski, E.; Kox, M. H. F.; Kornatowski, J.; Olsbye, U.; Weckhuysen, B. M. *Chem. - Eur. J.* **2008**, *14*, 11320−11327.
(37) Ristanović, Z.; Kubarev, A. V.; Hofkens, J.; Roeffaers, M. B. J.; Weckhuysen, B. M. *J. Am. Chem. Soc.* **2016**, *138*, 13586−13596.
(38) Liu, K.-L.; Kubarev, A. V.; Van Loon, J.; Uji-i, H.; De Vos, D. E.; Hofkens, J.; Roeffaers, M. B. J. *ACS Nano* **2014**, *8*, 12650−12659.
(39) Reichardt, C. *Solvents and Solvent Effects in Organic Chemistry*, 3rd ed.; Wiley-VCH Verlag GmbH & Co. KGaA: Weinheim, FRG, 2003; pp 471−507.
(40) Houlleberghs, M.; Hoffmann, A.; Dom, D.; Kirschhock, C. E. A.; Taulelle, F.; Martens, J. A.; Breynaert, E. *Anal. Chem.*, **2017**, under review.
(41) Hunger, M.; Kärger, J.; Pfeifer, H.; Caro, J.; Zibrowius, B.; Bülow, M.; Mostowicz, R. J. *J. Chem. Soc., Faraday Trans. 1* **1987**, *83*, 3459−3486.
(42) Hunger, M.; Freude, D.; Pfeifer, H.; Schwieger, W. *Chem. Phys. Lett.* **1990**, *167*, 21−26.

DOI: 10.1021/acscatal.7b00782
ACS Catal. 2017, 7, 4248−4252